American Mineralogist, Volume 71, pages 1502–1509, 1986

Cation ordering in the limited solid solution Fe_2SiO_4-Zn_2SiO_4

Tore Ericsson

Department of Mineralogy and Petrology, Institute of Geology, Uppsala University, Box 555, S-75122 Uppsala, Sweden

Anestis Filippidis

Department of Mineralogy and Petrology, University of Thessaloniki, G-54006, Thessaloniki, Greece

Abstract

Synthetic samples in the system Fe_2SiO_4 (fayalite structure, orthorhombic)–Zn_2SiO_4 (willemite structure, trigonal), equilibrated at 1000°C, were investigated by means of X-ray diffraction, scanning-electron microscope, microprobe, and Mössbauer spectroscopy (77–700 K).

The two-phase region is estimated to occur in the interval ~17–48 mol% of Zn_2SiO_4 at 1000°C and 0 bar. It is obvious from calculated densities that the fayalite structure is ~17% more dense at comparable compositions. The volumes per formula unit increase with Fe content in both phases, allowing the determination of the composition from X-ray diffraction data. The fayalite structure contains two octahedral metal positions M(1) (1 symmetry) and M(2) (*m* symmetry), and it is shown that Zn is preferentially occupying the M(1) site with $K_D \simeq 0.43$ and $\Delta G \simeq 8.9$ kJ/mol for samples equilibrated at 1000°C and quenched to room temperature. There are three tetrahedral-cation positions in Zn_2SiO_4 (willemite structure), Zn(1), Zn(2), and Si, and it is shown that Fe occupies the Zn positions in the willemite structure, with a preference for one of the positions. The obtained K_D and ΔG values (0.49 and 7.6 kJ/mol, respectively, at 1000°C and 0 bar), are nearly the same as the ones obtained for the fayalite structure.

Introduction

Studies by various methods of solid solution of transition elements in olivines (orthorhombic) showed that in forsterite the M(1) site is preferentially occupied by Ni (Rajamani et al., 1975; Walsh et al., 1976; Bish, 1981; Taftø and Spence, 1982), Co (Ghose and Wan, 1974; Walsh et al., 1976), and Zn (Ghose et al., 1975; Brown, 1982). On the other hand, Mn (Fujino, 1980; Francis and Ribbe, 1980; Taftø and Spence, 1982; Lumpkin et al., 1983) shows preference for the M(2) site.

In fayalitic olivines the preferences are the same as above for Ni (Annersten et al., 1982; Nord et al., 1982; Ribbe and Lumpkin, 1984), Co (pers. comm. with M. Jali, Institute of Geology, Uppsala University), and Mn (Brown, 1970; Shinno, 1980; Annersten et al., 1984). In the forsterite-fayalite solid solution, Mg and Fe enter the two sites in a nearly random way (Akimoto et al., 1976; Warburton, 1978; Taftø and Spence, 1982).

Introduction of Zn in fayalite gives only a partial solid solution: on the Zn-rich side, the structure is willemite (trigonal). In natural willemites, the most frequent substitutent for Zn is Mn and to a lesser degree Mg and Fe (Palache, 1935; Nysten, 1983).

On the whole, willemite is much less studied than the olivines. The Fe_2SiO_4-Zn_2SiO_4 solid-solution series has not been particularly studied either. To our knowledge, cation site preferences have not been determined, and the phase boundary between the two structures has not been established. The aim of this investigation is to clarify the phase relations and site occupancies. Such information may also contribute to a better understanding of the preferences observed in the olivine structure in general.

Crystal structure

Fayalite (Fe_2SiO_4) is orthorhombic with crystal symmetry *Pbnm* (no. 62 in *International Tables of Crystallography,* 1952) and contains four formula units per unit cell (Z = 4). At room temperature, the cell axes are a = 4.816, b = 10.469, and c = 6.099 Å (Birle et al., 1968). There are two octahedrally coordinated metal sites: M(1) and M(2). The M(1) octahedron has an inversion center, and M(2) lies on a mirror plane. The M(1) octahedron has an average metal–oxygen distance (⟨M(1)–O⟩) of 2.159 Å, whereas ⟨M(2)–O⟩ = 2.178 Å. The maximum deviation between the octahedral bond lengths is 0.105 Å for M(1) but 0.219 Å for M(2). Si occupies a tetrahedral position with ⟨Si–O⟩ = 1.638 Å (Birle et al., 1968). A projection of the crystal structure on the **a-c** plane is shown in Figure 1.

Willemite (Zn_2SiO_4) is trigonal ($R\bar{3}$ with hexagonal axes a = 13.948, c = 9.315 Å); Z = 18 (Klaska et al., 1978). There are three tetrahedrally coordinated cation sites: Zn(1), Zn(2), and Si. The three positions have ⟨Zn(1)–O⟩ = 1.950, ⟨Zn(2)–O⟩ = 1.961, and ⟨Si–O⟩ = 1.635. The maximum tetrahedral deviations are Zn(1)–O = 0.007, Zn(2)–O = 0.038, and Si–O = 0.015 Å (Klaska et al.,

0003–004X/86/1112–1502$02.00

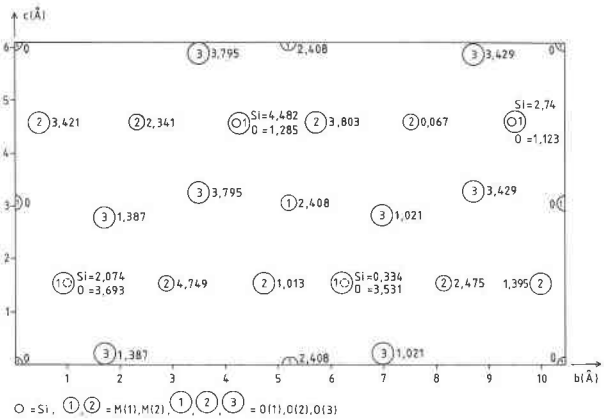

Fig. 1. A projection of the unit cell for fayalite on the **b**-**c** plane. Data from Birle et al. (1968).

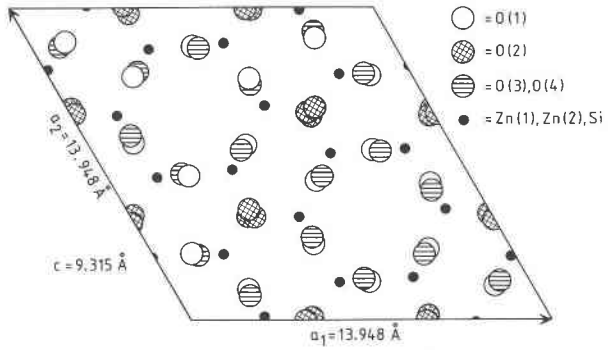

Fig. 2. A projection of the unit cell of willemite (hexagonal setting, Z = 18) on the **c** plane. Parameter values from Klaska et al. (1978).

1978). Other crystal-structure determinations with only minor differences in values compared to those above were made by Hang et al. (1970), Kodaira et al. (1975), and Simonov et al. (1978). A projection of the unit cell on the **c** plane in hexagonal setting is shown in Figure 2.

Sample preparation and experimental details

Sample preparation

Five synthetic samples of the system Fe_2SiO_4-Zn_2SiO_4 were produced from oxide mixtures (Fe_2O_3, 99.712%; ZnO, 99.944%; SiO_2, 99.89%). SiO_2 was obtained as quartz, crushed to 325 mesh and fired at 1000°C to remove absorbed water.

The mixtures were melted twice in an arc furnace using Ar as the protecting gas and afterward homogenized at 1000°C in evacuated SiO_2 tubes for two weeks. The tubes were quenched in water.

Characterization of sample purity and homogeneity

Polished and thin sections of each sample were examined petrographically in reflected and transmitted light. Phase analyses were obtained from X-ray powder diffraction, using Cu$K\alpha$ radiation and scanning interval 5–75° (2θ). Cell parameters of the phases were calculated from 14 to 18 different reflections using a computer program (CELNE). Au-plated pieces of the samples were observed using a JEOL JSM-U3 scanning-electron microscope (SEM) in reflection geometry. Al-coated samples were examined in scanning mode over several grains for homogeneity of Fe, Zn, and Si. Elemental analyses were performed by standard techniques at 20 kV using a Cambridge Geoscan spectrometer having a take-off angle of 75°. Pure metals (Fe and Zn) and natural olivines (Si) were used as standards. Six typically different grains were examined for each sample, and the obtained compositions were corrected for background, dead time, absorption, fluorescence, and atomic-number effects by using a computer program (MK 13).

Mössbauer measurements

Mössbauer spectroscopy data (^{57}Fe) were recorded between 77 K (using a liquid N_2 flow cryostat) and 704 K (using a vacuum furnace) in transmission geometry with an electromechanical Doppler velocity generator operating at constant acceleration mode in conjunction with a ND 1200 MCA (512 channels). The zero-setting and calibration of the velocity scale were made with a natural Fe foil at room temperature as the absorber, and the source was ^{57}Co diffused into a Rh matrix at high temperature. During the measurements, the source was kept at room temperature. The powder absorbers contained less than 5 mg/cm² of natural Fe. Owing to the thin absorbers used, the Lorentzian lines were used in the fitting procedure without any thickness correction. Since there was no indication of texture or Goldanskii-Karyagin effects in the samples (Ericsson and Wäppling, 1976), symmetrical doublets were used in the fitting procedure.

Results

Sample compositions and descriptions

The optical investigation of the homogenized samples revealed the presence along the grain boundaries of minute amounts of franklinite in samples W10, W11, and W12 and of magnetite in W13-F13 and F14 (W = willemite, F = fayalite structure). The magnetic phases were easily removed under acetone from the finely powdered samples by a hand magnet. The final identification of the magnetic phases was confirmed by X-ray, SEM, and microprobe analyses.

The crystal size of the synthetic olivines and willemites was large enough (>10 μm) to allow microprobe analyses of individual grains (Table 1), except for sample W13-F13 containing both phases. Sample W13-F13 was more fine-grained (~3 μm) compared to the other samples. Still the individual grains contained both phases, making an individual microprobe analysis of the two phases unreliable. No zoning or inhomogeneity was observed in any sample in the X-ray and microprobe analyses. X-ray and SEM analyses showed W10, W11, and W12 to be one-phase samples with willemite structure (Fig. 3) and F14 to be only one phase with fayalite structure (Fig. 4). The final compositions of the samples having willemite or fayalite structure deviated from the starting oxide mixtures owing to the removal of the magnetic phases, mentioned above. The Fe depletion in W10, W11, W12 was on the order of 20%, whereas the Zn depletion in F14 was ~5%. The cell parameters of the two structures as a function of composition are given in Table 1. The cell parameters increase with Fe content in the willemites (Fig. 5). Using the cell parameters and the compositional variations of

Table 1. Composition and cell parameters of the synthetic samples

	Willemite structure (hexagonal)				Fayalite structure (orthorhombic)		
	W10	W11	W12	W13	F13	F14	F17*
SiO_2 (wt%)	27.26	27.16	27.94			28.89	29.5
FeO (wt%)	3.32	16.78	28.11			65.79	71.8
ZnO (wt%)	69.42	56.05	43.96			5.32	0.0
Σ	100.00	99.99	100.01			100.00	101.3
	Number of ions on the basis of 4 oxygens						
Si	1.00	0.99	1.00	1.00	1.00	0.99	0.99
Fe^{2+}	0.10	0.51	0.84	1.04	1.66	1.88	2.02
Zn	1.89	1.51	1.16	0.96	0.34	0.13	0.00
X_{Fe}	0.05	0.25	0.42	0.52	0.83	0.94	1.00
X_{Zn}	0.95	0.75	0.58	0.48	0.17	0.06	0.00
	Cell parameters						
Structure	Hex	Hex	Hex	Hex	Orth	Orth	Orth
a (Å)	13.943(1)	13.955(1)	13.962(2)	13.980(4)	4.801(1)	4.820(2)	4.821(1)
b (Å)	—	—	—	—	10.471(1)	10.479(3)	10.478(2)
c (Å)	9.324(1)	9.366(1)	9.416(3)	9.429(6)	6.093(1)	6.083(3)	6.092(2)
V (Å^3)	1569.7(1)	1579.7(1)	1589.6(3)	1596.0(5)	306.3(1)	307.2(3)	307.7(2)
V (Å^3) per formula unit	87.21	87.76	88.31	88.66	76.58	76.80	76.93

Note: The relative errors are ±1.2% for ZnO, ±0.9% for FeO, and 10.5% for SiO_2. The figures in parentheses represent the estimated standard deviations (esd); thus 13.943(1) indicates an esd of 0.001.

* The values are from a synthetic sample (no. 17 in Annersten et al., 1982).

d_{333} and d_{113} reflections (Fig. 6) of the willemites, a rough estimate of W13 gave the composition $(Fe_{1.04}Zn_{0.96})SiO_4$. A similar extrapolation, using crystallographic data on samples F17 and F14, gave the composition of F13 to be $(Fe_{1.66}Zn_{0.34})SiO_4$. Thus the two-phase interval at 1000°C and 0 bar on the join Fe_2SiO_4-Zn_2SiO_4 is roughly from 52 to 83 mol% of Fe_2SiO_4 (synthesis boundaries and not reversed phase equilibria).

Mössbauer spectroscopy

The Mössbauer spectrum of fayalite in the paramagnetic region at room temperature or colder is characterized by two peaks; thus the signals emanating from Fe at the M(1) and M(2) positions are not resolvable. However, at temperatures above ~600 K, the centroid shift (CS) as well as the quadrupole splitting ΔE_Q (the peak separation

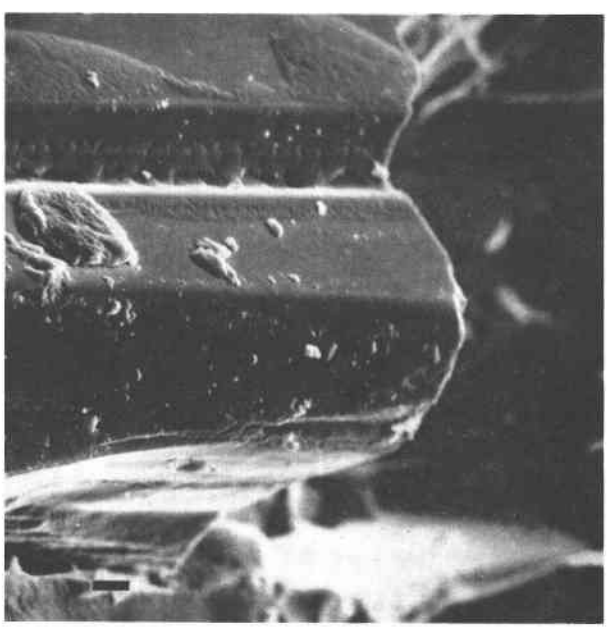

Fig. 3. Scanning-electron microphotograph of Fe-containing willemite (sample W10). Bar scale = 10 μm. The hexagonal **c** axis is in the plane of the photograph.

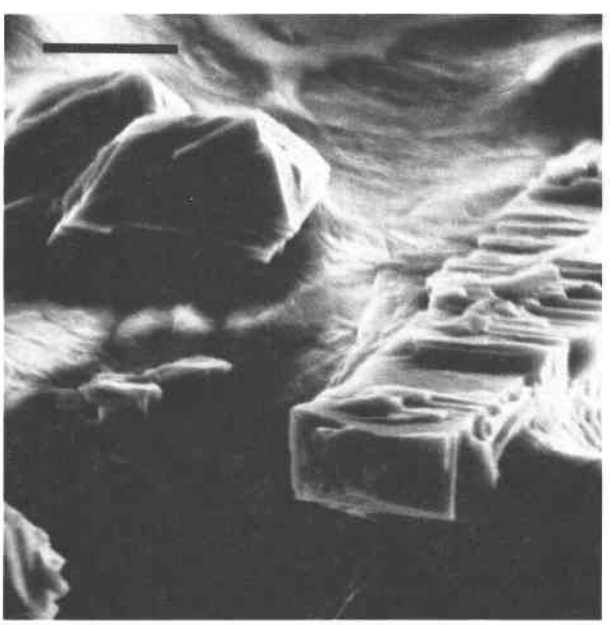

Fig. 4. Scanning-electron microphotograph of Zn-containing fayalite (orthorhombic shape). Sample F14. Bar scale = 10 μm.

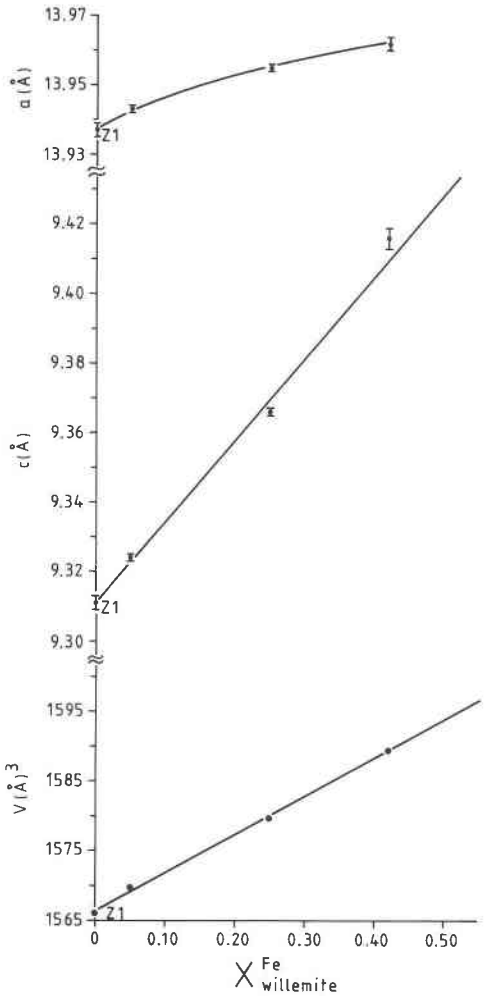

Fig. 5. Cell-parameter variations with composition of synthetic Fe-containing willemites. Z1 = average value from Klaska et al. (1978), Kodaira et al. (1975), Hang et al. (1970), and ASTM 8-492.

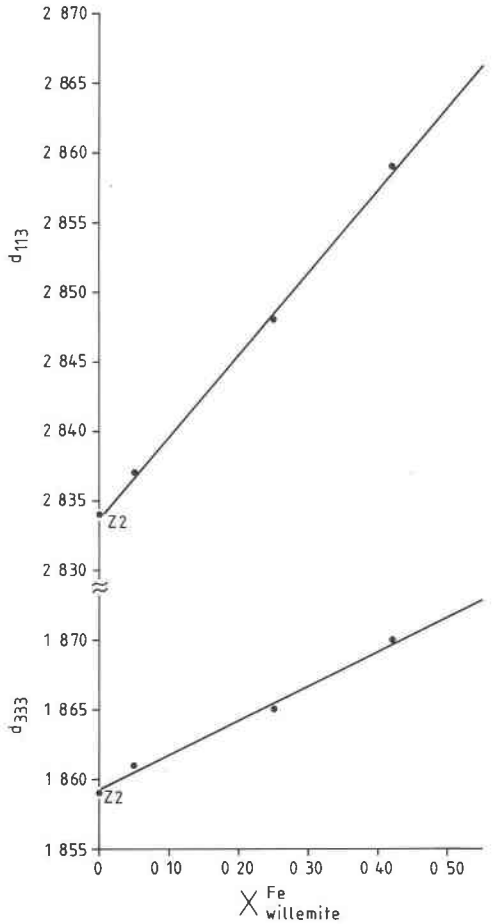

Fig. 6. Variations with composition of d_{333} and d_{113} in synthetic Fe-containing willemites. Z2 from ASTM 8-492.

in a doublet) for Fe at the two positions are significantly different resulting in partly resolved spectra (Fig. 7). The assignments of the two doublets are made in agreement with Annersten et al. (1982) and cited references therein: the doublet having the smaller quadrupole splitting corresponds to Fe at the M(1) site. According to Ingalls (1964) an increase in distortion normally results in a decrease in ΔE_Q for Fe^{2+}. Thus, the octahedral bond-length variation [0.105 Å for M(1) and 0.219 Å for M(2)] is not a relevant measure of octahedral distortion in fayalite. However, angle variations and other measures of distortions (Brown, 1970; Dollase, 1974; Fleet, 1974; Walsh et al., 1976) give M(1) as the more distorted octahedron. Moreover, if the octahedral bond-angle variance is used as a measure of distortion the M(1) distortion increases at a faster rate than the M(2) distortion with increasing temperature (Brown and Prewitt, 1973). The more pronounced decrease in ΔE_Q with increasing temperature for M(1) compared to M(2) is then in accordance with the Ingalls' theory as cited above. The obtained CS values at elevated temperatures are in accord with size considerations: the smaller M(1) site gives the smaller CS value; however, this crude rule does not give a clear difference in room-temperature spectra. Comparing the results with what we have obtained for pure fayalite (Annersten et al., 1982), it is obvious that Zn prefers the M(1) position. The Mössbauer parameters are collected in Table 2 for different compositions and temperatures.

Mössbauer spectra from the willemite region show features analogous to those in spectra of the fayalite phase. At room temperature and colder, they consist of only two absorption profiles (Fig. 8). However, at elevated temperatures, the absorption pattern can be attributed to two partly overlapping quadrupole doublets (Fig. 9) with a resolution not as distinct as in the fayalite phase.

At $T \simeq 700$ K, the obtained CS values are ~0.72 mm/s for the two doublets but ~0.82 for Fe at M(1) and ~0.90 for Fe at M(2) in the fayalite region. The lower CS values in the earlier case reflect the change in coordination numbers (CN): four in the willemite, but six in the fayalite region (Bancroft, 1974, p. 157). The similar CS values obtained for the two doublets in the willemite region, even

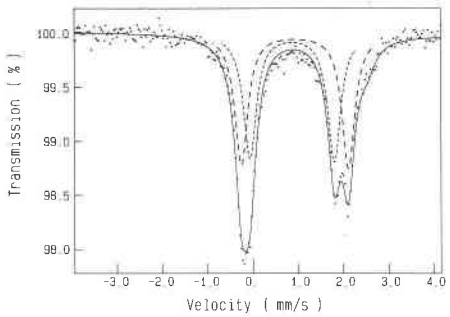

Fig. 7. Mössbauer spectrum of sample F14 $[(Fe_{0.94}Zn_{0.06})_2SiO_4]$ recorded at 627 K. The signal from Fe at M(1) is denoted by short dashed lines, Fe from M(2), having a larger quadrupole splitting, is denoted by long dashed lines. The full line is the sum of the fitted Lorentzian functions. (The absorption around 2.7 mm/s is from an impurity in the furnace having $CS/\Delta E_Q = 1.18/2.70$ mm/s.)

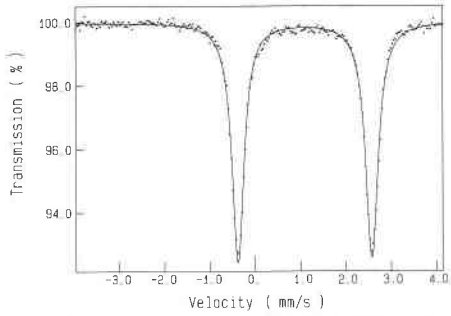

Fig. 8. Mössbauer spectrum of sample W12 $[(Fe_{0.42}Zn_{0.58})_2SiO_4]$ recorded at 77 K.

at elevated temperatures, suggest an assignment to two tetrahedral positions of nearly equal size: thus we assign the doublets to Fe occupying the Zn(1) and Zn(2) positions in the willemite structure but not to the smaller 4-coordinated Si position (see "crystal structure"). However, individual assignment of the two Zn positions cannot be made reliably from the $CS/\Delta E_Q$ values obtained. According to the theory of Ingalls (1964) and the bond-length variation as a measure of distortion, position 1 in Table 2 should correspond to Zn(2). However, the differences in bond lengths within the two positions are too small to make a conclusive decision. The Zn(1) position is somewhat smaller (0.011 Å according to Klaska et al., 1978), but as the CS of position 1 is approximately equal to the CS of position 2 even at elevated temperatures, this fact cannot be used for an assignment either.

Discussion

Cation preferences in the fayalite structure

The intracrystalline exchange of Fe and Zn in the fayalite structure can be expressed as

$$Zn^{2+}_{M1} + Fe^{2+}_{M2} \rightleftharpoons Zn^{2+}_{M2} + Fe^{2+}_{M1}.$$

The equilibrium constant at the characteristic temperature T is given by

$$K_{eq} = \frac{X_{Fe_{M1}} f_{Fe_{M1}} X_{Zn_{M2}} f_{Zn_{M2}}}{X_{Fe_{M2}} f_{Fe_{M2}} X_{Zn_{M1}} f_{Zn_{M1}}}.$$

$X_{Fe_{M1}}$, etc., are site-occupancy factors and $f_{Zn_{M1}}$, etc., are the partial activity coefficients for divalent Fe at M(1),

Table 2. Mössbauer parameters of $(Fe_{1-x}Zn_x)SiO_4$ recorded at different temperatures

			Position 1					Position 2					
Sample	X_{Fe}	T(K)	CS	ΔE_Q	W	Int.	X_{Fe}	CS	ΔE_Q	W	Int.	X_{Fe}	K_D
F17*	1.00	540	0.91	1.99	0.24	0.490	1.000	0.98	2.47	0.24	0.510	1.000	—
		673	0.83	1.76	0.24	0.490	1.000	0.90	2.25	0.24	0.510	1.000	—
F14	0.94	295	1.15	2.83	0.35	—	—	1.15	2.83	0.35	—	—	—
		519	0.94	2.17	0.29	0.473	0.907	1.03	2.58	0.29	0.527	0.973	0.27
		627	0.87	1.87	0.34	0.486	0.932	0.94	2.37	0.34	0.514	0.948	0.75
		629	0.84	1.82	0.31	0.484	0.929	0.91	2.30	0.31	0.516	0.951	0.67
F13	0.83	295	1.12	2.83	0.35	—	—	1.12	2.83	0.35	—	—	—
		501	0.93	2.19	0.47	0.434	0.737	1.01	2.60	0.47	0.566	0.923	0.23
		674	0.78	1.82	0.49	0.434	0.737	0.89	2.25	0.49	0.566	0.923	0.23
W12	0.42	77	1.10	2.95	0.33	—	—	1.10	2.95	0.33	—	—	—
		295	1.03	2.77	0.40	—	—	1.03	2.77	0.40	—	—	—
		592	0.78	1.65	0.46	0.366	0.315	0.81	2.41	0.40	0.634	0.525	0.42
		627	0.76	1.52	0.48	0.377	0.317	0.77	2.36	0.37	0.623	0.523	0.42
		704	0.72	1.45	0.41	0.363	0.313	0.72	2.25	0.35	0.637	0.527	0.41
W11	0.25	295	1.02	2.83	0.35	—	—	1.02	2.83	0.35	—	—	—
		433	0.91	2.14	0.45	0.390	0.195	0.89	2.70	0.30	0.610	0.305	0.55
		593	0.75	1.64	0.43	0.362	0.186	0.76	2.38	0.30	0.638	0.314	0.50
		687	0.74	1.49	0.40	0.389	0.1945	0.73	2.28	0.28	0.611	0.3055	0.55
W10	0.05	295	1.04	2.87	0.36	—	—	1.04	2.87	0.36	—	—	—
		695	0.71	1.52	0.40	0.363	0.037	0.74	2.25	0.33	0.637	0.063	0.57

Note: CS is given relative metallic Fe at room temperature, and ΔE_Q is the peak separation in the doublet. Precision is ±0.01 mm/s for CS and for full half-width at half maximum (W), ±0.02 mm/s for ΔE_Q, and ±0.02 for the intensities. The temperature stability was better than ±2 K. An underlined value is constrained, i.e., F14 at 295 K was fitted with only one doublet.

* The values for F17 are from Annersten et al. (1982).

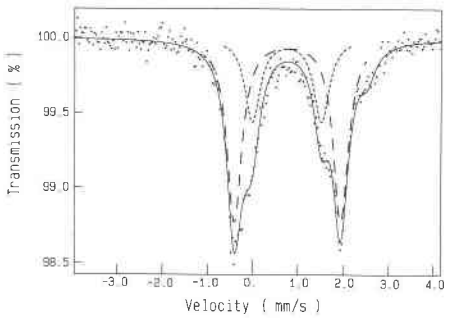

Fig. 9. Mössbauer spectrum of sample W12 [$(Fe_{0.42}Zn_{0.58})_2SiO_4$] recorded at 627 K. Fe at position 1 in Table 1 is denoted by short dashed lines, Fe at position 2 by long dashed lines. For further information, see caption to Fig. 7.

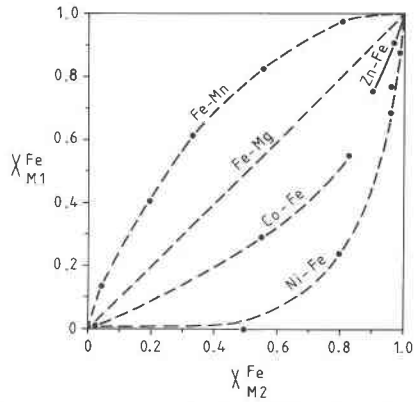

Fig. 10. Fe site occupancies in olivines (equilibration temperature, 1000°C): Ni-Fe from Annersten et al. (1982), Co-Fe from M. Jali (pers. comm.), Fe-Mg from Brown (1982), Mn-Fe from Annersten et al. (1984), Zn-Fe from this study.

etc. Ideal solid-solution conditions give activity coefficients equal to unity. Owing to the limited solid solution in the Zn_2SiO_4-Fe_2SiO_4 system, such conditions cannot be assumed to prevail here. Anyway, the cation-distribution coefficient K_D is a fair approximation of K_{eq} if the activity factors are reasonably close to unity:

$$K_D = \frac{X_{Fe_{M1}}(1 - X_{Fe_{M2}})}{X_{Fe_{M2}}(1 - X_{Fe_{M1}})}.$$

The K_D values obtained are presented in Table 2 and show a clear preference for Fe^{2+} to occupy the M(2) site (average $K_D \simeq 0.43$ in the interval studied). If $K_D \approx K_{eq}$, the change in Gibbs free energy ($\Delta G = -RT \ln K_D$) in a vacuum at 1000°C, assuming the annealing temperature to be the characteristic temperature, is ~8.9 kJ/mol (2.1 kcal/mol).

Substitution for Fe in the fayalite structure by transition metals other than Zn has been studied recently by other groups and by us, and the preferences are shown in Figure 10. The tendency to occupy the M(1) site compared to M(2) is given by the following sequence (ionic radius is below each ion):

$$\underset{0.69}{Ni^{2+}} > \underset{0.745\ 0.74}{(Co^{2+},Zn^{2+})} > \underset{0.72\ 0.78}{(Mg^{2+},Fe^{2+})} > \underset{0.83}{Mn^{2+}},$$

i.e., Ni^{2+} prefers M(1) in (Ni^{2+},Fe^{2+})-olivines, but Mn^{2+} prefers M(2) in (Mn^{2+}, Fe^{2+})-olivines and in (Mg^{2+}, Fe^{2+})-olivines there is a random ordering. One of the factors influencing the preferences is the radius of the different divalent cations, and therefore we have given the effective ionic radius in high-spin octahedral configuration below each element in the sequence above, according to Shannon (1976). As mentioned earlier, M(1) is smaller than M(2); thus the sequence found supports an assumption that the preferences are mainly governed by ionic radii (Mg^{2+} is an exception).

Cation preferences in the willemite structure

In spite of the structural change, the ordering of (Fe,Zn) is of the same strength in the Zn-containing fayalites and the Fe-containing willemites (Table 2). If size considerations prevail, Zn^{2+} being a smaller ion (0.60 Å compared to 0.63 Å for Fe^{2+} in 4-coordination; Shannon, 1976) should occupy the Zn(1) position, which is 0.011 Å smaller compared to the Zn(2) position (Klaska et al., 1978). Such an assignment corresponds to "position 1" being the Zn(1) position in Table 2. However, this assignment cannot be verified using $CS/\Delta E_Q$ values from Mössbauer spectroscopy as already mentioned.

The intracrystalline exchange of Fe and Zn in the willemite structure can be described as

$$Zn^{2+}_{\text{position 1}} + Fe^{2+}_{\text{position 2}} \rightleftharpoons Zn^{2+}_{\text{position 2}} + Fe^{2+}_{\text{position 1}}.$$

Following the same procedure as mentioned above, one can calculate cation-distribution coefficients valid for the willemite-phase samples.

The obtained K_D values (average, 0.49), if characteristic for the annealing conditions of 1000°C and 0 bar, correspond to a change in ΔG of ~7.6 kJ/mol (1.8 kcal/mol) with a preference for Fe^{2+} in "position 2" (Table 2).

Phase transition

The two-phase region obtained (~52–83 mol% of Fe_2SiO_4 in vacuum at 1000°C) is most likely sensitive to pressure. The volume per $(Zn,Fe)_2SiO_4$ unit is 88.66 Å^3 for W13 and 76.58 Å^3 for F13 (Table 1), indicating that the fayalite structure is a high-pressure polymorph. This is probably true for compositions near the two-phase region. For comparison, at 1200°C the solubility limit of Zn_2SiO_4 in the Mg_2SiO_4 olivine is ~75% at 90 kbar, but only ~24% at 1 bar (Syono et al., 1971). However, a high-pressure study, up to 170 kbar at temperatures up to 1500°C, of pure Zn_2SiO_4 revealed five high-pressure polymorphs, none being olivine-like (Syono et al., 1971).

Navrotsky (1973) made an extrapolation from solid-solution data to estimate the volume of Zn_2SiO_4, hypothetically having the fayalite structure, and got a volume increase of 17.2% when Zn_2SiO_4 transformed from fayalite to willemite structure. Using data in the same publication, it is possible to estimate a volume increase of ~19% when Fe_2SiO_4 transforms hypothetically from fayalite to willem-

ite structure. This is in good agreement with our data presented here, giving a volume increase of ~17% in the transition region.

The obtained two-phase region can also be used for making estimations of changes in Gibbs free energy when Fe_2SiO_4 hypothetically transforms from fayalite (fa) to willemite (wi) structure. Following a procedure proposed by Navrotsky and Kleppa (1967), the result is

$$\Delta G \simeq -2RT \ln (X^{wi}_{Fe}/X^{fa}_{Fe}) \simeq 9.90 \text{ kJ/mol} \quad (\simeq 2.36 \text{ kcal/mol});$$

when Zn_2SiO_4 hypothetically transforms from willemite to fayalite structure,

$$\Delta G \simeq -2RT \ln (X^{fa}_{Zn}/X^{wi}_{Zn} \simeq 21.97 \text{ kJ/mol} \quad (\simeq 5.25 \text{ kcal/mol}).$$

$X^{wi}_{Fe} = Fe/(Fe + Zn)$ in the willemite structure at the border to the two-phase region and so on. Such an estimate is very rough as it neglects deviations from ideality in the two solid solutions. Navrotsky (1980) estimated (from activity data) $\Delta G = 10.5$ kcal/mol when Zn_2SiO_4 hypothetically transformed from willemite to fayalite structure at 1 bar and 1323 K. Our estimation above gives a much lower value. However, it seems as though most of the deviation is due to the rough model used. Using the same model, the value of 10.5 kcal/mol corresponds to $X^{fa}_{Zn}/X^{wi}_{Zn} = 0.14$, i.e., a much smaller solubility of Zn in the fayalite structure than we actually measure at 1273 K.

Acknowledgments

We are grateful to Professor K. Soldatos, University of Thessaloniki, for his kind interest in our work, to Professor G. Christofides at the same university for critically reading the manuscript, to Christina Wernström for drawing the figures, and to Hans Harryson, who performed the microprobe measurements. We are also thankful to Michael Jali, who let us use his data on Co-Fe olivines prior to publication. Finally, we also want to thank Professor Alexandra Navrotsky, who as a referee proposed many clear improvements of the original manuscript.

Financial support for this study was partly obtained from the Swedish Natural Science Research Council (NFR).

References

Akimoto, S., Matsui, Y., and Syono, Y. (1976) High-pressure crystal chemistry of orthosilicates and the formation of the mantle transition zone. In R.G.J. Strens, Ed. The physics and chemistry of minerals and rocks, 327–363. Wiley, London.

Annersten, H., Ericsson, T., and Filippidis, A. (1982) Cation ordering in Ni-Fe olivines. American Mineralogist, 67, 1212–1217.

Annersten, H., Adetunji, J., and Filippidis, A. (1984) Cation ordering in Fe-Mn silicate olivines. American Mineralogist, 69, 1110–1115.

Bancroft, G.M. (1974) Mössbauer spectroscopy. McGraw-Hill, New York.

Birle, J.D., Gibbs, G.V., Moore, P.B., and Smith, J.V. (1968) Crystal structures of natural olivines. American Mineralogist, 53, 807–824.

Bish, D.L. (1981) Cation ordering in synthetic and natural Ni-Mg olivines. American Mineralogist, 66, 770–776.

Brown, G.E. (1970) The crystal chemistry of olivines. Ph.D. thesis. Virginia Polytechnic Institute and State University, Blacksburg.

——— (1982) Olivines and silicate spinels. Mineralogical Society of America Reviews in Mineralogy, 5, 2nd edition, 275–381.

Brown, G.E., and Prewitt, C.T. (1973) High temperature crystal chemistry of hortonolite. American Mineralogist, 58, 577–587.

Dollase, W.A. (1974) A method for determining the distortion of coordination polyhedra. Acta Crystallographica, A30, 513–517.

Ericsson, T., and Wäppling, R. (1976) Texture effects in 3/2–1/2 Mössbauer spectra. Journal de Physique, 37, Colloque C6, 719–723.

Fleet, M.E. (1974) Distortions in the coordination polyhedra of M site atoms in olivines, clinopyroxenes, and amphiboles. American Mineralogist, 59, 1083–1093.

Francis, C.A., and Ribbe, P.H. (1980) The forsterite-tephroite series I. Crystal structure refinements. American Mineralogist, 65, 1263–1269.

Fujino, Kiyoshi. (1980) Crystal chemistry of Mn-Mg-Fe olivine solid solution series (in Japanese with English abs.). Mineralogical Society of Japan Journal, 14 (special issue 3), 135–143.

Ghose, S., and Wan, C. (1974) Strong site preference of Co^{2+} in olivine $Co_{1.10}Mg_{0.90}SiO_4$. Contributions to Mineralogy and Petrology, 47, 131–140.

Ghose, S., Wan, C., Okamura, F.P., Ohashi, H., and Weidner, J.R. (1975) Site preference and crystal chemistry of transition metal ions in pyroxenes and olivines. Acta Crystallographica, A31, Suppl. S76.

Hang, C., Simonov, M.A., and Below, N.V. (1970) Crystal structures of willemite Zn_2SiO_4 and its germanium analogue Zn_2GeO_4. Soviet Physics Crystallography, 15, 387–390.

Ingalls, R.I. (1964) Electric field gradient tensor in ferrous compounds. Physical Review, 133A, 787–795.

International tables for X-ray crystallography. (1952) Vol. 1, 151. Kynoch Press, Birmingham, England.

Klaska, K.H., Eck, J.C., and Pohl, D. (1978) New investigation of willemite. Acta Crystallographica, B34, 3324–3325.

Kodaira, K., Ito, S., and Matsushita, T. (1975) Hydrothermal growth of willemite single crystals in acidic solutions. Journal of Crystal Growth, 29, 123–124.

Lumpkin, G.R., Ribbe, P.H., and Lumpkin, N.E. (1983) Composition, order-disorder and lattice parameters of olivines: Determinative methods for Mg-Mn and Mg-Ca silicate olivines. American Mineralogist, 68, 1174–1182.

Navrotsky, Alexandra. (1973) Thermodynamic relations among olivine, spinel and phenacite structures in silicates and germanates: I. Volume relations and the systems NiO-MgO-GeO_2 and CoO-MgO-GeO_2. Journal of Solid State Chemistry, 6, 21–41.

——— (1980) Lattice stability of AX and AB_2O_4 compounds. Calphad, 4, 255–264.

Navrotsky, A., and Kleppa, O.J. (1967) The thermodynamics of cation distributions in simple spinels. Journal of Inorganic and Nuclear Chemistry, 29, 2701–2714.

Nord, A.G., Annersten, H., and Filippidis, A. (1982) The cation distribution in synthetic Mg-Fe-Ni olivines. American Mineralogist, 67, 1206–1211.

Nysten, Per. (1983) A willemite-bearing paragenesis from Långban. Geologiska Föreningens i Stockholm Förhandlingar, 105, 273–274.

Palache, Charles. (1935) The minerals of Franklin and Sterling Hill, N.J. U.S. Geological Survey Professional Paper 180, 1–135.

Rajamani, V., Brown, G.E., and Prewitt, C.T. (1975) Cation ordering in Ni-Mg olivine. American Mineralogist, 60, 292–299.

Ribbe, P.H., and Lumpkin, G. R. (1984) Cation ordering in Ni-Fe olivines: Corrections and discussion. American Mineralogist, 69, 161–163.

Shannon, R.D. (1976) Revised effective ionic radii and systematic studies of interatomic distances in halides and chalcogenides. Acta Crystallographica, A32, 751–761.

Shinno, Isamu. (1980) Relations between (130) spacing, chemical composition and cation site preference of olivine. Japanese Association of Mineralogists, Petrologists and Economic Geologists Journal, 75, 343–352.

Simonov, M.A., Sandomirskii, P.A., Egorov-Tismenko, Yu.K., and Belov, N.V. (1978) The crystal structure of willemite Zn_2SiO_4. Soviet Physics Doklady, 22, 622–623.

Syono, Y., Akimoto, S.-I., and Matsui, Y. (1971) High pressure transformations in zinc silicates. Journal of Solid State Chemistry, 3, 369–380.

Taftø, J., and Spence, J.C.H. (1982) Crystal site location of iron and trace elements in a magnesium-iron olivine by a new crystallographic technique. Science, 218 (4567), 49–51.

Walsh, D., Donnay, G., and Donnay, J.D.H. (1976) Ordering of transition metal ions in olivine. Canadian Mineralogist, 14, 149–150.

Warburton, D.L. (1978) Mössbauer effect studies of olivines. Ph.D. thesis, University of Chicago, Chicago, Illinois.

Manuscript received October 2, 1985
Manuscript accepted July 8, 1986